Mixing in Fluids

Undergraduate Honors Thesis

Miranda Mundt

Mentor: Dr. Monika Nitsche

University of New Mexico Department of Mathematics and Statistics

January 7, 2015

Acknowledgements

I would like to thank my mentor Dr. Monika Nitsche for her unshakable support, not only for our project, but for all the Research Experience for Undergraduate (REU) participants. Her enthusiasm for students and their betterment through the Mentoring through Critical Transition Points (MCTP) program is unparalleled, from outreach programs to travel arrangements for research conferences.

I would also like to thank the National Science Foundation (NSF) for their continued support through the NSF-MCTP Grant, NSF Award DMS-1148801.

Abstract

This is scenario for our problem: there is a finite flat plate immersed in a parallel horizontal background flow, hinged at the leading edge. Above the plate is red fluid and below the plate is blue fluid. The free end of the plate oscillates about the horizontal axis in a prescribed periodic fashion. As fluid moves past the plate, a boundary layer of vorticity is formed and separates from the free end. The separated shear layer rolls up into consecutive vortices of opposite sign, one vortex per stroke of the plate. We model this system using the Euler equations, which do not include the effects of viscoscity, the "stickiness" of a fluid. Because of this, we would not have boundary layer separation. This aspect of viscous flow is modelled by shedding point vortices parallel from the trailing edge of the plate at every time step, imposing the Kutta condition upon each point. The shed vorticity is modelled by a regularized vortex sheet attached to the trailing tip of the plate. The plate is modelled by a bound vortex sheet whose strength is determined at each time step such that no flow goes through the wall and circulation remains constant using Kelvin's theorem. We then implement the fourth-order Runge Kutta method to progress the system at every time step. T computational results consist of the shed vortex sheet at a sequence of times, with red particles above the sheet and blue below. We estimate the amount of mixing by averaging the amount of blue and red particles in boxes of size $2h$. Results are presented for different values of h, and show that there is a larger proportion of red particles in every other vortex. We also observe the displacement of individual fluid particles in a reference frame fixed at infinity and determine that there are interesting patterns within the vortex showing regions in which particles have returned to their original positions. Results also show that the integral displacement $V_d(t) = \iint_R d(\mathbf{x}_0, t) d\mathbf{x}_0$ of fluid particles moving through the flow past the plate increases as a function of time, seemingly without leveling off. In the future, we want to complete a longer run simulation in order to see if over extended periods of time, the distance function eventually hits a plateau.

Contents

Chapter 1

Introduction

With the realization of the importance of climate change research, there is an increased interest in the effect of mixing in water sources, particularly oceans, and its effect on nutrient movement and temperature change. A recent article from *Nature* details the efforts of a pair of scientists to measure the level of mixing induced by the motion of sea creatures [2]. They found that for large sea creatures, the amount of biogenic mixing induced is a significant contributor to ocean mixing and nutrient transport. With this research in hand, one is inclined to ask, then, how much mixing actually occurs?

This is the inspiration for our current research. We wish to find a mathematical measure of the intensity of mixing as a fish swims through fluid at rest far away, such as in a fish bowl. We have chosen to study the problem in a reference frame fixed on the fish, and model the fish by an oscillating flat plate. The plate is immersed in a parallel horizontal background flow, hinged at the leading edge. Above the plate is one color fluid (i.e., red) and below is a different color fluid (i.e., blue). The free end of the plate oscillates about the horizontal axis in a prescribed periodic fashion. As fluid moves past the plate wall, a boundary layer of vorticity is formed and separates from the free end. The separated shear layer rolls up into a vortex, but with every oscillation of the plate, the vorticity in the shear layer changes sign. Thus the shed vorticity rolls up into a set of vortices of opposite sign. Refer to Figure 1.1 for a visual.

Our question is how much this motion mixes the blue and red fluids. In order to determine the answer to this, we first develop a mathematical model based on Euler's equations to mimic this phenomenon. The parts of the model include approximating the plate by a bound vortex sheet, approximating the flow by a free vortex sheet, and approximating the separation of vorticity via the Kutta condition. We neglect the diffusion of viscoscity within the model, so we have a sharp difference in velocity across the free sheet rather than a smooth transition. In the following sections, we will

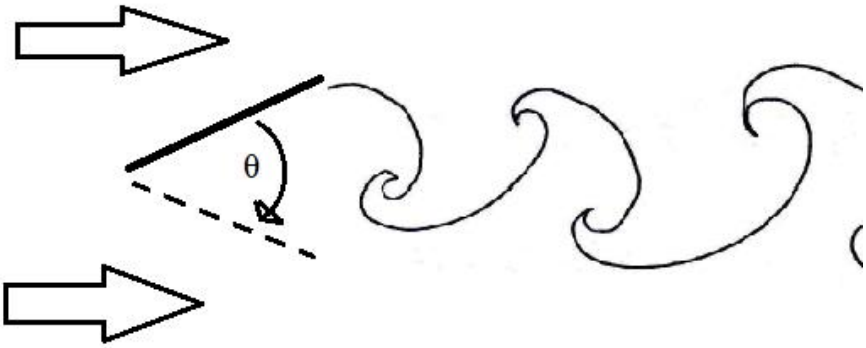

Figure 1.1: Visual of the Model

discuss in detail the parts of the model.

We then develop a measure of proportion of mixing using a coarse and fine grid of points laid over the flow. The coarse grid is used as the corner of boxes, within which we use the fine grid to measure the proportion of red fluid particles to total fluid particles. This gives us a level of mixing, and using different sized coarse grids allows us to explore different levels of mixing. In addition to this, we then investigate the displacement over time of particles in a large "slab" of points. In a reference frame fixed at infinity, we track the displacement of the particles within the slab of fluid as the plate travels through. We quantify this displacement in two ways. First, we plot the total displacement of each particle for a sequence of times. Second, we compute the integral displacement of all particles in the slab as a function $V_d(t)$. This function appears to grow based on our data, but appears to be approaching a plateau. Ideally, we would like to complete a longer run simulation to see if this is truly a plateau or if this function continues to grow.

The thesis is organized as follows. Chapter 2 describes the background of the problem. Chapter 3 describes the results of our mixing analysis. Chapter 4 describes the results of the displacement analysis. Chapter 5 summarizes the results and describes future research directions.

Chapter 2

Background

In this chapter, we will detail the background that contributes to the construction of our model[1].

2.1 Vorticity

Let $\mathbf{u} = (u, v, w, t)$ be the velocity vector field of the fluid flow. Then the vorticity is defined as the curl of the velocity: $\boldsymbol{\omega} = \nabla \times \mathbf{u} = (w_y - v_z, u_z - w_x, v_x - u_y)$. Vorticity is the rotation of a fluid - like water in a sink or bathtub as it is let out through the drain. Taylor series shows that the fluid velocity is locally approximated by the superposition of a translation (constant velocity) plus irrotational strain field (irrotation means zero vorticity) plus rotating flow that rotates in the plane normal to the vorticity vector with angular velocity equal to half the magnitude of the vorticity vector. In a two-dimensional flow in the (x, y) plane, we have that $w = 0$ and $\frac{\partial}{\partial z} = 0$. As a result, $\boldsymbol{\omega} = (0, 0, v_x - u_y)$, so the vorticity points in the z direction. The nonzero component $v_x - u_y$ is referred to as the scalar vorticity. Our oscillating plate flow is assumed to be two dimensional. Refer to Figure 2.1.

Circulation around a given curve, denoted Γ_C, is given by equation (2.1). Using Stokes Theorem, we see that $\Gamma_C = \int \omega dA$, or in our case, $\Gamma_C = \int (v_x - u_y) dx dy$.

$$\Gamma_C = \oint_C \mathbf{u} \cdot d\mathbf{s} = \int_0^L \mathbf{u} \cdot \mathbf{T} ds = \int \omega dA. \tag{2.1}$$

For a single vortex, which we call a point vortex, we have that $\omega = \Gamma \delta(x, y)$. Basically, this vortex is modelled by a delta function. A delta function is a function which is zero everywhere except at the origin, where the function is so large that its integral value is nonzero. Thus the flow induced by a point vortex at the origin has zero vorticity everywhere outside

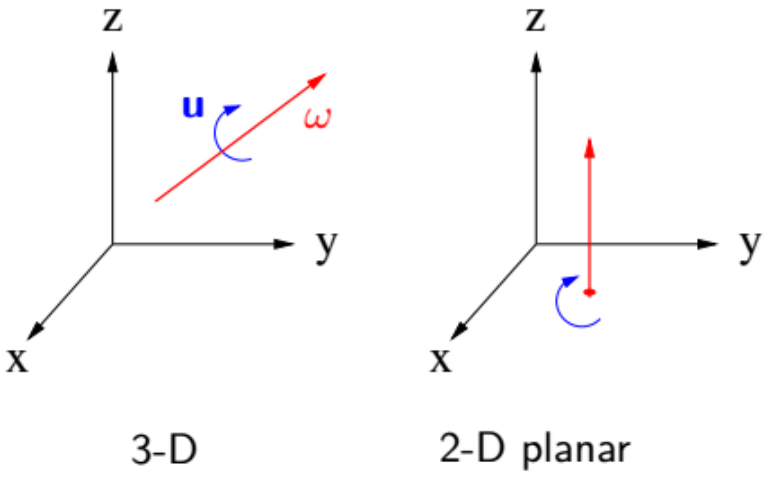

Figure 2.1: Sample Vorticity Vectors

the origin, but it has nonzero total circulation. The induced velocity is given by equation (2.2)[6].

$$(u, v) = \frac{\Gamma}{2\pi} \frac{(-y, x)}{x^2 + y^2} \tag{2.2}$$

In complex notation, associating the complex number $z = x + iy$ with the point (x, y) in the plane, we can write the conjugate complex velocity as

$$\begin{aligned} u - iv &= \frac{-\Gamma}{2\pi} \frac{(y + ix)}{x^2 + y^2} \\ &= \frac{\Gamma}{2\pi i} \frac{(x - iy)}{x^2 + y^2} \\ &= \frac{\Gamma}{2\pi i} \frac{1}{x + iy} \\ &= \frac{\Gamma}{2\pi i z}. \end{aligned} \tag{2.3}$$

Point vortices are an essential part of our model. We use them for the plate and for the flow that is induced by the plate. This will be covered in later sections.

2.2 Euler and Navier-Stokes

In this section, we will discuss Euler's and Navier-Stokes' equations, including their contribution to our model. We will start with their inspiration, as it comes from common physical principles. There are three equations

which make up both Euler and Navier-Stokes systems: one based on conservation of mass, one on conservation of momentum, and one on conservation of energy. We will begin with mass to follow the derivation by Chorin and Marsden [1].

In the derivations below, we often refer to the following theorem and its generalization to higher dimensions, stated here without proof.

Theorem 1. ***Leibniz Formula*** *If f is a continually differentiable function in $[a,b]$ (i.e., $f \in C^1[a,b]$), then $\frac{d}{dt}\int_a^b f(t,s)ds = \int_a^b \frac{\partial}{\partial t} f(t,s)ds$. See [5], page 324.*

2.2.1 Euler Equations

The first equation follows the conservation of mass, the law which states that mass is neither created or destroyed. There are two versions of this equation. The first is the integral form:

$$\frac{d}{dt}\int_W \rho dV = -\int_{\partial W} \rho \mathbf{u}\cdot\mathbf{n} dA \tag{2.4}$$

where W is a fixed subregion of fluid, with smooth boundary ∂W, and $\rho(\mathbf{x},t)$ is the mass density. Here, $\mathbf{n}$ is the outward pointing normal to W. This equation states that the rate of increase of mass in W equals the rate at which mass is crossing ∂W in the inward direction. By the divergence theorem, which states that over a given region S and its piecewise smooth boundary ∂S with positive origin, $\int\int_{\partial S} \mathbf{F}\cdot d\mathbf{S} = \int\int\int_S div\mathbf{F} dV$ where $\mathbf{F}$ is C^1, we can rewrite equation (2.4) as $\int_W \left[\frac{\partial \rho}{\partial t} + div(\rho\mathbf{u})\right] dV = 0$. Because this equation is to hold for every W, we can again rewrite it as:

$$\frac{\partial \rho}{\partial t} + div(\rho\mathbf{u}) = 0. \tag{2.5}$$

or, by the identity $\nabla(f\mathbf{F}) = f(\nabla\cdot\mathbf{F}) + \mathbf{F}\cdot\nabla f$, where $f = \rho$ and $\mathbf{F} = \mathbf{u}$,

$$\begin{aligned} \frac{\partial \rho}{\partial t} + \rho\nabla\cdot\mathbf{u} + \mathbf{u}\cdot\nabla\rho = 0 \\ \frac{D\rho}{Dt} + \rho\nabla\cdot\mathbf{u} = 0 \end{aligned} \tag{2.6}$$

where $\frac{D\rho}{Dt} = \frac{\partial\rho}{\partial t} + \mathbf{u}\cdot\nabla\rho$. This is called the differential form of the conservation of mass, or the continuity equation. In this equation, we see that if the divergence of $\rho\mathbf{u}$ is positive, then there is compression in the system. The reverse, when the divergence of $\rho\mathbf{u}$ is negative, leads to expansion.

The second equation is based on the balance of momentum. The physical property behind this equation is the law that every action (or force) must have an equal and opposite reaction in a closed system. That is, in a closed

system, the total momentum is constant. In the Euler equations, this second equation is:

$$\rho \frac{D\mathbf{u}}{Dt} = -\nabla p + \rho \mathbf{b} \tag{2.7}$$

where $\frac{D}{Dt} = \partial_t + \mathbf{u} \cdot \nabla$ is the material derivative, $p(\mathbf{x}, t)$ is the pressure, and $\mathbf{b}(\mathbf{x}, t)$ are the body forces per unit mass. This equation can also be compared to Newton's second law, which states that force is the same as mass times acceleration. In our model, we drop the extraneous body forces, so our equation is simplified to $\rho \frac{D\mathbf{u}}{Dt} = -\nabla p$.

The final equation is actually split between two types of flow: incompressible, where the material density is constant within a fluid particle or, alternatively, the divergence of the velocity vector field is 0; and isentropic, which is compressible and characterized by the existence of a function w such that $\nabla w = \frac{1}{\rho} \nabla p$. Our flow is incompressible and so we will look in more detail at this version.

In incompressible flow, it is assumed that all of the energy in the system is kinetic energy and that the rate of change of kinetic energy in a portion of fluid equals the rate at which the pressure and body forces do work. That is, $\frac{d}{dt} E_{kinetic} = -\int_{\partial W_t} p\mathbf{u} \cdot \mathbf{n} dA + \int_{W_t} \rho \mathbf{u} \cdot \mathbf{b} dV$. Because of incompressibility (i.e., $div(\mathbf{u}) = 0$) and the divergence theorem, we see that this is the same as $-\int_{W_t} (\mathbf{u} \cdot \nabla p - \rho \mathbf{u} \cdot \mathbf{n}) dV$, but this is a consequence of the balance of momentum equation. Thus, we have that in incompressible flows, the Euler equations are:

$$\begin{aligned} \rho \frac{D\mathbf{u}}{Dt} &= -\nabla p \\ \frac{D\rho}{Dt} &= 0 \\ div(\mathbf{u}) &= 0 \end{aligned} \tag{2.8}$$

with the boundary condition that no fluid goes through wall boundaries of the fluid, i.e.,

$$\mathbf{u} \cdot \mathbf{n} = \mathbf{u}_{wall} \cdot \mathbf{n}. \tag{2.9}$$

2.2.2 Navier-Stokes Equations

The Navier-Stokes' equations are similar to the Euler equations with two distinct differences: the balance of momentum equation and an additional boundary condition. If we recall equations (2.8), the second is the balance of momentum for incompressible flows. In Navier-Stokes, however, we have a diffusion term brought on by viscosity. This term comes about from the natural "stickiness" or "thickness" of a fluid, such as honey, which has a much higher viscosity than water. Physically, honey will stick to a wall as it moves past in a visible layer, whereas water has less resistance and will

have a very thin boundary layer. The equation is:

$$\frac{D\mathbf{u}}{Dt} = -\nabla\left(\frac{p}{\rho_0}\right) + \frac{\mu}{\rho_0}\triangle\mathbf{u} \tag{2.10}$$

where ρ_0 is a constant density and $\frac{\mu}{\rho_0}$ is the coefficient of kinematic viscosity, which is responsible for diffusion within the system.

The extra boundary condition for Navier-Stokes completes the system of equations and is consistent with physical observations: no flow at the wall. It leads to boundary layer formation. To define, a boundary layer forms in a thin layer of fluid near a wall as the velocity decreases, eventually becoming 0 at the wall. In equation form, this condition is $\mathbf{u} = 0$ at the wall. This is called the "no-slip condition". As a result, the velocity on the wall becomes zero. Since the effect of viscosity is to resist, the velocity close to the wall continuously decreases, while away from the wall the velocity is equal to that of the fluid flow. Thus a layer with a velocity gradient establishes itself close to the wall . This is the boundary layer. All together, we have that the Navier-Stokes equations for homogeneous flow (constant density $\rho = \rho_0$) are:

$$\begin{aligned} \frac{D\mathbf{u}}{Dt} &= -\nabla\left(\frac{p}{\rho_0}\right) + \frac{\mu}{\rho_0}\triangle\mathbf{u} \\ div(\mathbf{u}) &= 0 \end{aligned} \tag{2.11}$$

with the boundary conditions that $\mathbf{u} = 0$ at the walls and $\mathbf{u} \cdot \mathbf{n} = 0$.

2.3 Shear Layer

A shear layer is a region of a flow where there is a significant velocity gradient, or where tangential velocity changes sharply, across a border, such as at the boundary of a wall. This in particular is called a boundary layer. As the flow gets closer to the wall, the velocity slows down, eventually reaching 0 at the wall itself. Refer to Figure 2.2.

Realistically, this is what will happen when flow is approaching the flapping plate. As flow gets close to the plate, the viscoscity, or "stickiness" of the fluid, increases, and a boundary layer will form. This causes the velocity to slow to almost zero near the plate and actually zero at the wall. Once past the plate, the boundary layer will separate, which causes trailing concentrations of vortices to form. This flow can be simplified using the Euler equations, which we discussed in more detail in Section 2.2. Our hypothesis is that within these vortices, significant mixing occurs.

2.4 On Circulation in Inviscid, Homogeneous Flows

Definition 1. *The **circulation** around a closed curve C_t is defined: $\Gamma_{C_t} = \oint_{C_t} \mathbf{u} \cdot d\mathbf{s}$[1].*

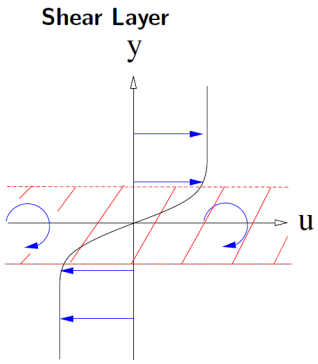

Figure 2.2: Free Shear Layer in the Interior of a Fluid

Definition 2. *A **vortex sheet** or **vortex line** is a surface S or a curve L that is tangent to the vorticity vector $\boldsymbol{\omega}$ at each of its points[1].*

Definition 3. *A **vortex tube** consists of a two-dimensional surface S, bounded by a curve C, that is nowhere tangent to $\boldsymbol{\omega}$, with vortex lines drawn through each point of C[1].*

Lemma 1. *Let $\mathbf{u}$ be the velocity field of a flow and C a closed loop with $C_t = \phi_t(C)$ a loop transported by the flow. Then $\frac{d}{dt}\int_{C_t} \mathbf{u} \cdot d\mathbf{s} = \int_{C_t} \frac{D\mathbf{u}}{Dt} d\mathbf{s}$.*

Proof. Let $\mathbf{x}(s)$ be a parametrization of the loop C, $0 \leq s \leq 1$. Then a parametrization of C_t is $\phi(\mathbf{x}(s), t)$ such that $\frac{\partial \phi}{\partial t} = \mathbf{u}$. By definition of the line integral,

$$\frac{d}{dt}\int_{C_t} \mathbf{u} \cdot d\mathbf{s} = \frac{d}{dt}\int_0^1 \mathbf{u}(\phi(\mathbf{x}(s), t), t) \cdot \frac{\partial}{\partial s}\phi(\mathbf{x}(s), t) ds.$$

Because our dependence is now on s, we can now move the $\frac{d}{dt}$ inside the integral. Using the product rule, we now have

$$\begin{aligned}
\frac{d}{dt}\int_{C_t}\mathbf{u}\cdot d\mathbf{s} &= \int_0^1 \frac{\partial}{\partial t}\left[\mathbf{u}(\phi(\mathbf{x}(s),t),t)\right]\cdot\frac{\partial}{\partial s}\phi(\mathbf{x}(s),t)\\
&+ \mathbf{u}(\phi(\mathbf{x}(s),t),t)\cdot\frac{\partial}{\partial t}\frac{\partial}{\partial s}\phi(\mathbf{x}(s),t)ds\\
&= \int_0^1\left[\frac{\partial}{\partial t}\mathbf{u}+\frac{\partial}{\partial x}\mathbf{u}\frac{dx}{dt}+\frac{\partial}{\partial y}\mathbf{u}\frac{dy}{dt}+\frac{\partial}{\partial z}\mathbf{u}\frac{dz}{dt}\right]\cdot\frac{\partial}{\partial s}\phi(\mathbf{x}(s),t)\\
&+ \mathbf{u}(\phi(\mathbf{x}(s),t),t)\cdot\frac{\partial}{\partial t}\frac{\partial}{\partial s}\phi(\mathbf{x}(s),t)ds\\
&= \int_0^1\left[\frac{\partial}{\partial t}\mathbf{u}+(\mathbf{u}\cdot\nabla)\mathbf{u}\right]\cdot\frac{\partial}{\partial s}\phi(\mathbf{x}(s),t)\\
&+ \mathbf{u}(\phi(\mathbf{x}(s),t),t)\cdot\frac{\partial}{\partial t}\frac{\partial}{\partial s}\phi(\mathbf{x}(s),t)ds\\
&= \int_0^1\frac{D\mathbf{u}}{Dt}(\phi(\mathbf{x}(s),t),t)\cdot\frac{\partial}{\partial s}\phi(\mathbf{x}(s),t)ds\\
&+ \int_0^1\mathbf{u}(\phi(\mathbf{x}(s),t),t)\cdot\frac{\partial}{\partial t}\frac{\partial}{\partial s}\phi(\mathbf{x}(s),t)ds.
\end{aligned}$$

where, by convention, $\frac{D}{Dt}$ denotes the material derivative $\frac{D}{Dt}=\frac{\partial}{\partial t}+\mathbf{u}\cdot\nabla$. By definition, $\frac{\partial\phi}{\partial t}=\mathbf{u}$, so the second term becomes

$$\int_0^1\mathbf{u}(\phi(\mathbf{x}(s),t),t)\cdot\frac{\partial}{\partial s}\mathbf{u}(\phi(\mathbf{x}(s),t),t)ds=\frac{1}{2}\int_0^1\frac{\partial}{\partial s}(\mathbf{u}\cdot\mathbf{u})ds.$$

Because C_t is closed, we get that the second term equals zero. Changing out of the parametrization to the original coordinate system, the first term equals

$$\int_{C_t}\frac{D\mathbf{u}}{Dt}ds.$$

□

Theorem 2. ***Kelvin*** *For isentropic flow without external forces, the circulation Γ_{C_t} is constant in time.*

Proof. Using the lemma and that the flow is isentropic, inviscid flow, with no external forces, (i.e., $\frac{D\mathbf{u}}{Dt}=-\nabla w$),

$$\begin{aligned}
\frac{d}{dt}\Gamma_{C_t} &= \frac{d}{dt}\oint_{C_t}\mathbf{u}\cdot d\mathbf{s}\\
&= \oint_{C_t}\frac{D\mathbf{u}}{Dt}d\mathbf{s}\\
&= -\oint_{C_t}\nabla w\cdot d\mathbf{s}\\
&= 0
\end{aligned}$$

because C_t is closed. □

Theorem 3. ***Helmholtz*** *If ρ is constant, then (1) If C_1 and C_2 are any two curves encircling a vortex tube, then $\oint_{C_1} \mathbf{u} \cdot d\mathbf{s} = \oint_{C_2} \mathbf{u} \cdot d\mathbf{s} = \Gamma$, and we call this common value the strength of the tube. (2) The strength of the vortex tube is constant in time as the tube moves with the fluid.*

Proof. Let C_1 and C_2 be as in Figure 2.3. The surface connected by these two curves is labeled S, and the end faces enclosed by C_1 and C_2 are labeled S_1 and S_2, respectively. The region enclosed by the curves and S is denoted by V, and $\Sigma = S \cup S_1 \cup S_2$. By Gauss' theorem, which states that $\iint_R \nabla \cdot \mathbf{F} d\mathbf{V} = \int_{\partial R} \mathbf{F} \cdot d\mathbf{A}$, we have

$$\begin{aligned} 0 &= \int_V \nabla \cdot \boldsymbol{\omega} dx = \int_\Sigma \boldsymbol{\omega} \cdot d\mathbf{A} \\ &= \int_{S_1 \cup S_2} \boldsymbol{\omega} \cdot d\mathbf{A} + \int_S \boldsymbol{\omega} \cdot d\mathbf{A} \\ &= \int_{S_1} \boldsymbol{\omega} \cdot d\mathbf{A} + \int_{S_2} \boldsymbol{\omega} \cdot d\mathbf{A} + \int_S \boldsymbol{\omega} \cdot d\mathbf{A}. \end{aligned}$$

Because each part of this equation must equal zero, then we know that $\int_{S_1} \boldsymbol{\omega} \cdot d\mathbf{A} = -\int_{S_2} \boldsymbol{\omega} \cdot d\mathbf{A}$. By Stokes' theorem, however, we know both

$$\begin{aligned} \int_{C_1} \mathbf{u} \cdot d\mathbf{s} &= \int_{S_1} \boldsymbol{\omega} \cdot d\mathbf{A} \\ \int_{C_2} \mathbf{u} \cdot d\mathbf{s} &= -\int_{S_2} \boldsymbol{\omega} \cdot d\mathbf{A} \end{aligned}$$

and since the right hand sides are equal, the first part of the theorem is proven. The second part follows as a direct result from Kelvin's theorem. □

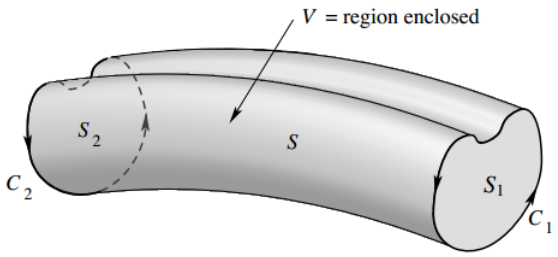

Figure 2.3: Image taken from [1].

2.5 The Vortex Sheet Approximation

In simulations, shear layers are difficult to model. For simplicity, we will approximate this shear layer with a vortex sheet. A vortex sheet is a surface of zero thickness characterized by a jump discontinuity in tangential velocity, rather than a diminishing velocity close to the wall, and can be viewed as an infinite sum of point vortices. Refer to Figure 2.4.

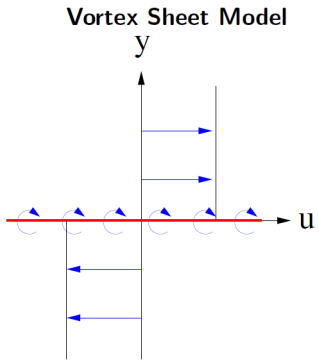

Figure 2.4: Example of a Vortex Sheet

To parametrize this sheet, we must utilize Kelvin's theorem. The following subsections will describe in more detail.

2.5.1 Birkhoff-Rott Equations

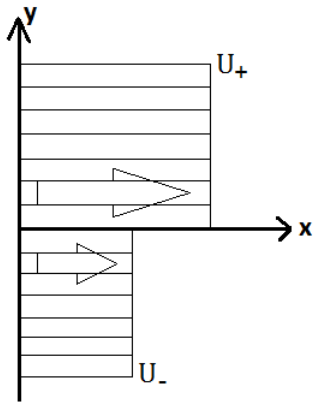

Figure 2.5: Jump Discontinuity in Velocity

The velocity of this free vortex sheet is given by the Birkhoff-Rott equations, which simply state that the sheet is given by an infinite superposition of point vortices. That is, if $z(\Gamma, t) = x(\Gamma, t) + iy(\Gamma, t)$, where $z(\Gamma, t)$ describes the vortex sheet position, with flow of a simple point vortex described by equation (2.3), parameterized by circulation Γ, then the velocity is given by the principal value integral, denoted by a dash through the integral sign:

$$\frac{d\bar{z}}{dt} = \frac{1}{2\pi i} \fint \frac{d\Gamma'}{z(\Gamma, t) - z(\Gamma', t)} = \frac{\overline{u_+ + u_-}}{2}. \tag{2.12}$$

where u_+ is the velocity above the sheet and u_- the velocity below the sheet, as in Figure 2.5. This second equality follows from the Plemelj relation, which is not shown here. For our approximation, we discretize this by $z_j(t) = z(\Gamma_j, t)$ and get

$$\frac{d\bar{z}_j}{dt} = \frac{1}{2\pi i} \sum_{k=1, k\neq j}^{N} \frac{\Delta\Gamma}{z_j - z_k}. \tag{2.13}$$

The function $\sigma(s)$ is called the vortex sheet strength. Referring to Figure 2.6 for a visual, we can define the following:

$$\begin{aligned} \Delta\Gamma &= \int_{\Delta C} \mathbf{u} \cdot ds \\ &\approx -u_+ \Delta s + u_- \Delta s \\ &= -(u_+ - u_-)\Delta s. \end{aligned}$$

So we see that

$$\frac{\Delta\Gamma}{\Delta s} \approx -(u_+ - u_-) = -[u]_-^+ = \sigma(s). \tag{2.14}$$

We call this the strength.

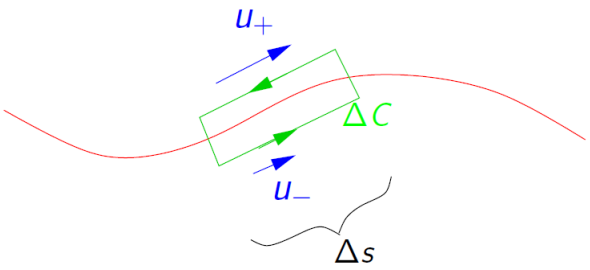

Figure 2.6: Vortex Sheet Visual

2.5.2 Instability

We now have to consider the possibility of an instability, however. We start with equation (2.12). We multiply the top and the bottom by $\overline{z(\Gamma,t)-z(\Gamma',t)}$, replace $z(\Gamma,t)=x+iy$ and $z(\Gamma',t)=x'+iy'$, and receive the following equations:

$$\begin{aligned}\frac{dx}{dt}&=\frac{-1}{2\pi}\int\frac{y-y'}{(x-x')^2+(y-y')^2}d\Gamma'\\ \frac{dy}{dt}&=\frac{1}{2\pi}\int\frac{x-x'}{(x-x')^2+(y-y')^2}d\Gamma'\end{aligned}\tag{2.15}$$

Consider a small perturbation of a flat sheet in the form $x(\Gamma,t)=\Gamma+p(\Gamma,t)$, $y(\Gamma,t)=\Gamma+q(\Gamma,t)$ where $p=Pe^{\omega t}e^{ik\Gamma}$ and $q=Qe^{\omega t}e^{ik\Gamma}$, and p, q are small, $O(\epsilon)$. Then we get

$$\begin{aligned}x-x'&=\Gamma-\Gamma'+p(\Gamma,t)-p(\Gamma',t)=\Gamma-\Gamma'+p-p'\\ y-y'&=q(\Gamma,t)-q(\Gamma',t)=q-q'.\end{aligned}\tag{2.16}$$

From here we get

$$(x-x')^2+(y-y')^2=(\Gamma-\Gamma')^2+2(\Gamma-\Gamma')(p-p')+O(\epsilon^2).\tag{2.17}$$

Then we see that

$$\begin{aligned}\frac{1}{(x-x')^2+(y-y')^2}&=\frac{1}{(\Gamma-\Gamma')^2+2(\Gamma-\Gamma')(p-p')+O(\epsilon^2)}\\ &=\frac{1}{(\Gamma-\Gamma')^2}\left[\frac{1}{1+\frac{2(p-p')}{\Gamma-\Gamma'}+O(\frac{\epsilon^2}{(\Gamma-\Gamma')^2})}\right].\end{aligned}\tag{2.18}$$

Using the Taylor expansion of $\frac{1}{1-x}$ where $x=-\frac{2(p-p')}{\Gamma-\Gamma'}-O(\frac{\epsilon^2}{(\Gamma-\Gamma')^2})$, we get

$$\frac{1}{1+\frac{2(p-p')}{\Gamma-\Gamma'}+O(\frac{\epsilon^2}{(\Gamma-\Gamma')^2})}=1-\frac{2(p-p')}{\Gamma-\Gamma'}-O\left(\frac{\epsilon^2}{(\Gamma-\Gamma')^2}\right)+O(\epsilon^4)\tag{2.19}$$

so then (2.18) becomes

$$\frac{1}{(x-x')^2+(y-y')^2}=\frac{1}{(\Gamma-\Gamma')^2}\left[1-\frac{2(p-p')}{\Gamma-\Gamma'}+O(\epsilon^2)\right].\tag{2.20}$$

We then multiply (2.20) by $x-x'$ and do some algebra to get:

$$\frac{x-x'}{(x-x')^2+(y-y')^2}=\frac{1}{\Gamma-\Gamma'}-\frac{p-p'}{(\Gamma-\Gamma')^2}+O(\epsilon^2).\tag{2.21}$$

From here we get the linearized equations, dropping the smaller terms:

$$\begin{aligned}\frac{dx}{dt} &= \frac{-1}{2\pi}\int \frac{q-q'}{(\Gamma-\Gamma')^2}d\Gamma' \\ \frac{dy}{dt} &= \frac{1}{2\pi}\int \frac{1}{\Gamma-\Gamma'} - \frac{p-p'}{(\Gamma-\Gamma')^2}d\Gamma' \\ &= \frac{-1}{2\pi}\int \frac{p-p'}{(\Gamma-\Gamma')^2}d\Gamma'.\end{aligned} \tag{2.22}$$

The first term in the second integral goes to zero, so it is dropped out and the formula for $\frac{dy}{dt}$ simplifies.

Plugging in our values for p and q into $\frac{dx}{dt}$ from (2.22),

$$\begin{aligned}P\omega e^{\omega t}e^{ik\Gamma} &= \frac{-1}{2\pi i}\int \frac{Qe^{\omega t}(e^{ik\Gamma}-e^{ik\Gamma'})}{(\Gamma-\Gamma')^2}d\Gamma' \\ P\omega &= \frac{-1}{2\pi i}\int \frac{Q(1-e^{ik(\Gamma'-\Gamma)})}{(\Gamma-\Gamma')^2}d\Gamma' \\ &= \frac{-Q}{2\pi}\int_{-\infty}^{\infty} \frac{1-e^{ikx}}{x^2}dx \\ &= \frac{Qk}{2}.\end{aligned} \tag{2.23}$$

This last equality follows from the residue theorem. Similarly, we can determine that $Q\omega = \frac{Pk}{2}$. Then we multiply the two results together and get

$$\begin{aligned}PQ\omega^2 &= PQ\frac{k^2}{4} \\ \omega^2 &= \frac{k^2}{4} \\ \omega &= \pm\frac{k}{2}.\end{aligned} \tag{2.24}$$

This is our dispersion relation. This dispersion presents us with two problems. First, we get exponential growth of high wavenumbers being introduced by roundoff. That is, once we decrease past machine precision, roundoff error is present in the system, which creates the potential for exponential growth of w. The second problem comes in the form of a singularity formation in finite time - that is, after some critical time t_c, this filter no longer works, so there will be no convergence of our point vortex approximation and k will continue to grow infinitely. We will cover the proposed solution to both of these problems in the next section.

2.5.3 Regularization

We must ask ourselves why the problems presented above are important. Machine accuracy can be significantly affected by the introduction of spurious roundoff error as it combines upon itself with each progessive timestep.

"When an analytic function is interpolated at equidistant points in exact arithmetic, the discrete Fourier coefficients decay exponentially with increasing wavenumber" but roundoff error can actually make these coefficients increase[3]. This creates irregular point motion, the likes of which is not seen in real flows. This roundoff error only increases with the number of intervals. Robert Krasny completed a study in 1986 which shows that for $N = 50$ equally spaced interpolation points, there is a relatively small amount of irregular point motion. For $N = 100$, however, irregular point motion appears early and increases exponentially due to compounded roundoff error. Because of this, one is unable to use any large values of N, thus becoming unable to achieve any increased accuracy in interpolation.

Robert Krasny presented a method of correction for the instabilities presented by the Birkhoff-Rott discretizations in 1986[3]. The first of these methods is to impose a filter upon the system which, below a certain machine representation level, any Fourier coefficient will be automatically set to 0 rather than be allowed to decrease below machine precision, thus causing artificial computational noise. For example, we could say that any coefficient below 10^{-13} be set to 0. This method is referred to as the "Krasny filter".

There is an outstanding issue with the Krasny filter, however – it only works before the time that a singularity forms in the flow. In our case, we have a singularity immediately, so we can never implement the Krasny filter. How, then, do we fix our flow such that we get regular point motion and roll up? The answer was also given by Krasny[4]. Instead of a filter which only works before the critical time t_c, this method works from the very beginning. He implements a regularization to the Birkhoff-Rott equations to desingularize them. He introduces a small $\delta > 0$ and receives the equation:

$$\frac{d\bar{z}}{dt} = \frac{1}{2\pi i}\int \frac{\overline{z(\Gamma,t) - z(\Gamma',t)}d\Gamma'}{|z(\Gamma,t) - z(\Gamma',t)|^2 + \delta^2} \tag{2.25}$$

with the discretization

$$\frac{d\bar{z}_j}{dt} = \frac{1}{2\pi i}\sum_{k=1,k\neq j}^{N} \frac{\overline{z_j - z_k}\Delta\Gamma}{|z_j - z_k|^2 + \delta^2}. \tag{2.26}$$

This equation produces convergence in N and δ past the critical time which, before, was unable to be passed, and allows for the creation of the "spiral" like appearance of real flows. Krasny's analysis revealed accurate and low-error, with high resolution, roll up. Thus, this discretization in equation (2.26) is the one present in our model.

2.6 Modelling Flow Past an Oscillating Plate

Using all of the pieces from previous sections, we will now describe our model in detail. Our model consists of three main parts: the free and bound vortex

sheet, the boundary layer separation, and our numerical approach

2.6.1 The Free Sheet

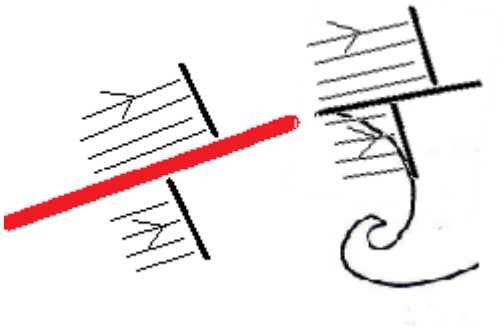

Figure 2.7: Free Vortex Sheet

The separated shear layer is modelled by a free vortex sheet. Its induced velocity is regularized, given by equation (2.26).

2.6.2 The Bound Sheet

The plate is modelled by a vortex sheet bound to the plate whose strength $\sigma(s)$ is determined such that the fluid velocity does not cross the plate. To recall from Section 2.2 on the Euler and Navier-Stokes equations, the first part is given by the formula $\mathbf{u} \cdot \mathbf{n} = \mathbf{u}_{wall} \cdot \mathbf{n}$. The plate is approximated by a sum of point vortices of strength $\Delta\Gamma_k$ that induce velocity given by equation (2.13).

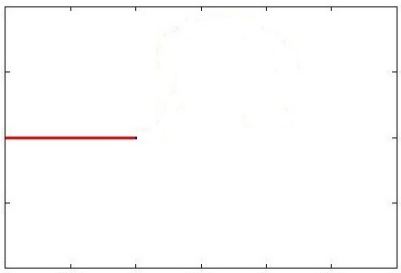

Figure 2.8: Bound Vortex Sheet

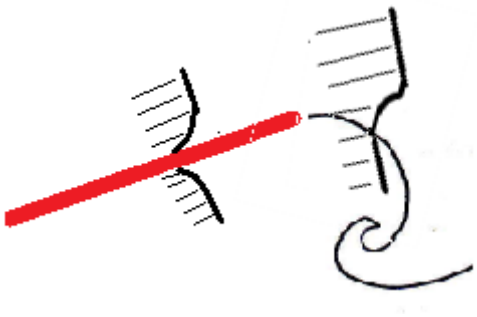

Figure 2.9: Boundary Layer Separation

2.6.3 Modelling Boundary Layer Separation

The next part of the model is releasing point vortices into the flow to simulate the boundary layer separation which is absent in the Euler equations. In this process, we have to determine two criteria: first where to place the vortices and second with what circulation. The "where" is given as parallel to the edge of the plate with the average veocity of u_- and u_+. We must invert the system given by $\sigma_{edge} = -(u^e_+ - u^e_-)$ and $u_{average,edge} = \frac{u^e_+ + u^e_-}{2}$ to determine this. The second determines that the circulation must be forced to adhere to the Kutta Condition.

Theorem 4. ***Kutta Condition*** *In inviscid, incompressible flow, satisfying the inviscid Euler Equations (refer to* (2.8)*), with fluid leaving parallel to the edge, the amount of vorticity shed from an edge satisfies* $\frac{d\Gamma}{dt} = \frac{1}{2}(u^2_- - u^2_+)$.

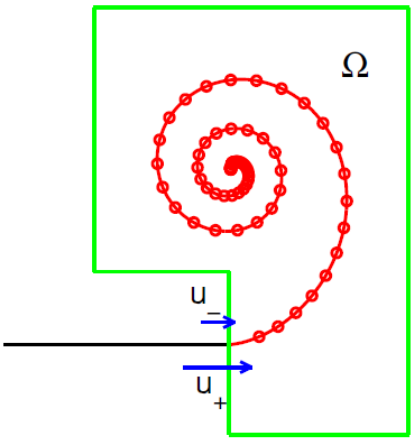

Figure 2.10: Shedding Off Plate - Kutta Condition

Proof. Refer to Figure 2.10 for a visual. We know by definition that $\Gamma(t) = \oint_\Omega \omega dV$. Then from the Euler equations

$$\begin{aligned}\frac{d\Gamma}{dt} &= \frac{d}{dt}\oint_\Omega \omega dV \\ &= \oint_\Omega \frac{\partial \omega}{\partial t} dV.\end{aligned}$$

From incompressibility and the identity $\nabla(f\mathbf{F}) = f(\nabla \cdot \mathbf{F}) + (\nabla f) \cdot \mathbf{F}$ where f is a scalar function and $\mathbf{F}$ is a vector function, it follows that, using $f = \omega$ and $F = \mathbf{u}$

$$\begin{aligned}\oint_\Omega \frac{\partial \omega}{\partial t} dV &= -\oint_\Omega (\mathbf{u} \cdot \nabla)\omega dV \\ &= -\oint_\Omega \nabla \cdot (\omega \mathbf{u}) dV.\end{aligned}$$

Then using the divergence theorem,

$$-\oint_\Omega \nabla \cdot (\omega \mathbf{u}) dV = -\oint_{\partial\Omega} \omega \mathbf{u} \cdot \mathbf{n} dS.$$

We assume from this point, for simplicity, that we have a reference frame in which the plate is parallel to the x-axis. Because of this, it follows that

$$\begin{aligned}-\oint_{\partial\Omega} \omega \mathbf{u} \cdot \mathbf{n} dS &= -\oint_{\partial\Omega} \frac{\partial u}{\partial y} u dy \\ &= -\oint_{\partial\Omega} \frac{1}{2}\frac{\partial (u^2)}{\partial y} dy \\ &= \frac{1}{2}(u_-^2 - u_+^2).\end{aligned}$$

□

Together, the Kutta condition, the strength, and the average velocity at the edge restrictions determine the vortex shedding, which is essential to each progressive time step.

2.6.4 Numerical Method

Nitsche and Krasny[7] developed the model described above to simulate axisymmetric flow out of a circular tube. Sheng et al.[8] applied this model to planar flow past the oscillating plate, as considered in this work. Our model must be updated at each time step using fourth-order Runge Kutta in states, as follows:

(1) Compute the sheet strength σ so that the fluid velocity normal to the plate is equal to the plate's normal velocity. This is achieved by determining the plate's position at time t, then calculating the right hand side of a system

$A\mathbf{x} = \mathbf{b}$, where $\mathbf{b}$ is the velocity, accounting for that induced by the plate, and $\mathbf{x}$ is σ.

(2) Evolve the system parts:

(a) free sheet using $\frac{dx}{dt} = \mathbf{u}_{freesheet} + \mathbf{u}_{plate}$, where $\mathbf{u}_{plate}$ uses the updated σ

(b) Γ using the Kutta condition, as described in 2.6.3

(c) plate (i.e., bound sheet) using $\frac{dx_{plate}}{dt} = \mathbf{u}_{plate}$.

After every stage within Runge-Kutta, (1) and (2) are both updated. After all stages of Runge-Kutta are completed, the vortex locations on the sheet and plate are updated as well as the time and σ. Then an insert routine is initiated (if necessary) to add extra points on the free sheet if two neighboring points are too far apart, the definition of "too far" being determined by the user at initialization.

See Figure 2.11 for the complete model, where the green is the plate, the blue is the vortex sheet, and the background lines are instantaneous streamlines (added in post-processing).

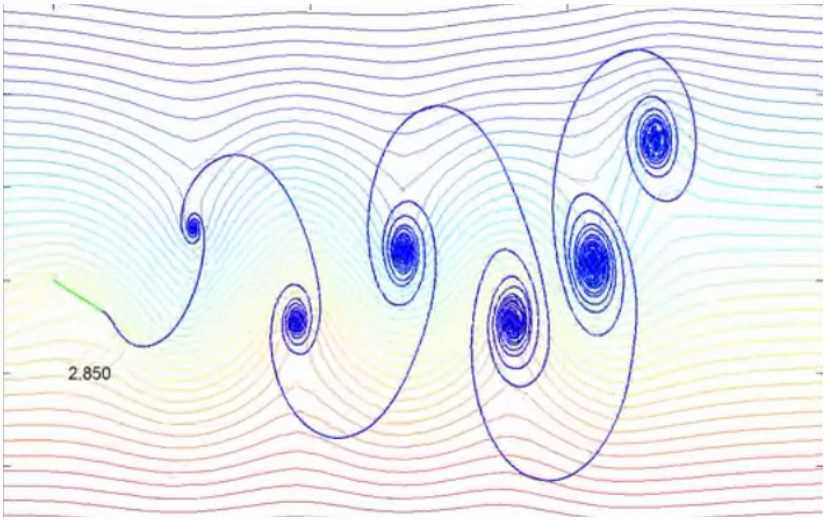

Figure 2.11: Complete Model

Chapter 3

Mixing Results

Our first goal of this project is to determine the degree to which fluid mixes when a fish swims past. Now that we have created the model of the physical system, we can actually begin to conduct our analysis. We require a few more steps before we can ultimately measure our mixing, though.

3.1 Set-Up

After running our code in FORTRAN, we have an output file in MATLAB format. We load the data into MATLAB and then introduce two grid point meshes on top of the calculated flow: a fine mesh and a coarse mesh. The coarse mesh will be used as corners of "boxes" around the elements within the fine mesh, where the parameter h defines half the side length of the "box". At each point of the fine mesh, we position a particle and determine whether this particle is "red" or "blue". Then we count the proportion of red particles in each of the boxes of the coarse mesh and assign this value to the center point of the coarse mesh.

To assign "red" and "blue", we must complete some simple calculations. First, for a point $f_0(x, y)$ in the fine mesh, we must find the point $x_s(x, y)$ on the sheet which is closest. Once we have found this closest point, we then create two vectors $\mathbf{V}_1$ and $\mathbf{V}_2$. The formulas are:

$$\begin{aligned} \mathbf{V}_1 &= x_{s+1} - x_s \\ \mathbf{V}_2 &= f_0 - x_s \end{aligned} \tag{3.1}$$

where x_{s+1} is the next point on the sheet in order of progression. We then take the cross product of these vectors. This will result in a vector which points only in the z direction. If the nonzero entry is negative, then f_0 is on the left side of the sheet and is assigned red. Otherwise, f_0 is blue.

We repeat this process for all of the points in the fine mesh. We then create a matrix with binary entries where each point is represented with either 1 or 0 (red or blue, respectively). We now incorporate the coarse

mesh. As stated earlier, we use the coarse mesh as corners on boxes which surround the points in the fine mesh.

First we pick four points from the coarse mesh that are arranged in a box and determine which fine mesh points reside inside of the corners. We isolate these entries from the binary matrix and sum them. We then divide this number, denoted R, by the total number of entries taken from the binary matrix, denoted T. This gives us a proportion, denoted M, of red points to total points within each box. As an example, say that the box created by our coarse mesh contains 12 points of the fine mesh. If 3 of the contained points are red, then the proportion would be 0.25.

3.2 Measuring Mixing

Using the process described in 3.1 with different size coarse grids, we generate several matrices of mixing proportions. Images are shown in Figure 3.1. (Larger images are shown at the end of the section.)

Each row of images in Figure 3.1 refers to a different size coarse grid, where h quantifies half the side length of the box. For example, (a) and (b) use $h = 0.1$, so the box used in these images has side length 0.2.

These images tell us a great deal about the intensity of mixing. As expected, mixing only truly occurs in the vortices as particles from above and below the sheet roll up with the sheet (though they do not cross, as will be discussed in 4.2). We also see that as h approaches zero, the smearing caused by the mixing shrinks considerably and the image reverts to that of just the vortex sheet.

Not as expected, however, is what happens within a vortex pair. As one can see, the left vortex of this pair clearly shows a larger proportion of blue particles whereas the right vortex clearly has more red particles. The case seems to be the same for every vortex pair. One vortex will clearly dominate in a certain color. We theorize that this is due to movement bias caused by the plate. That is, when the plate moves downward, there will be a larger amount of red particles present to be rolled into the sheet. The opposite is true when the plates moves upward - there will be a larger amount of blue particles.

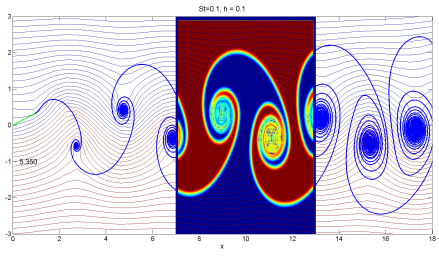

(a) Mixing, h=0.1

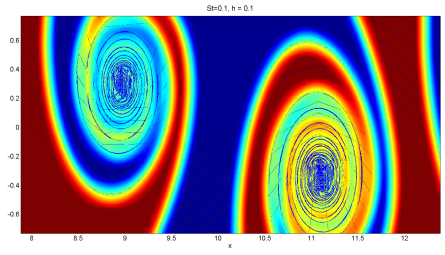

(b) Mixing, h=0.1, zoom

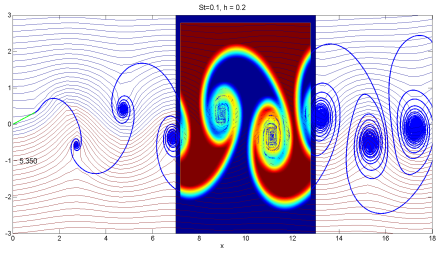

(c) Mixing, h=0.2

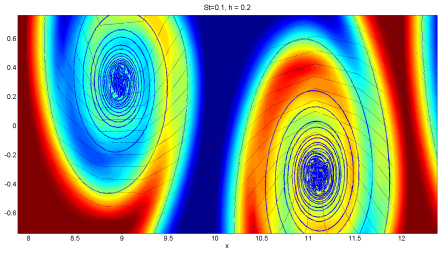

(d) Mixing, h=0.2, zoom

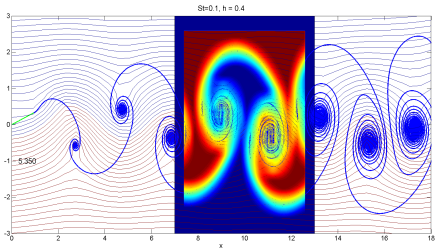

(e) Mixing, h=0.4

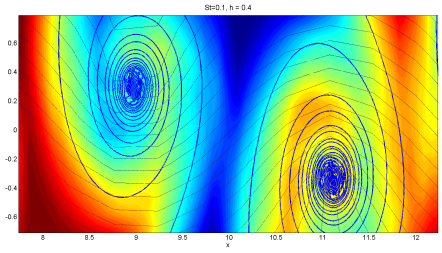

(f) Mixing, h=0.4, zoom

Figure 3.1: Mixing Results

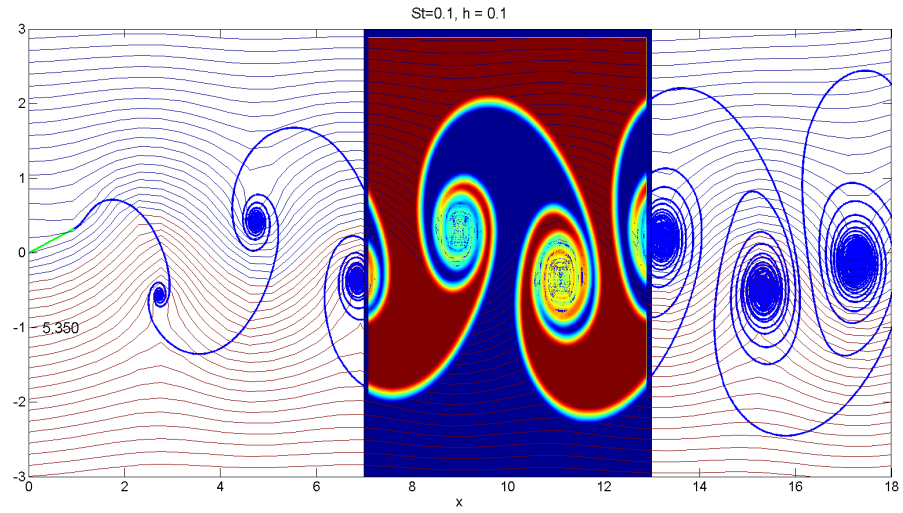
St=0.1, h = 0.1
5.350
x

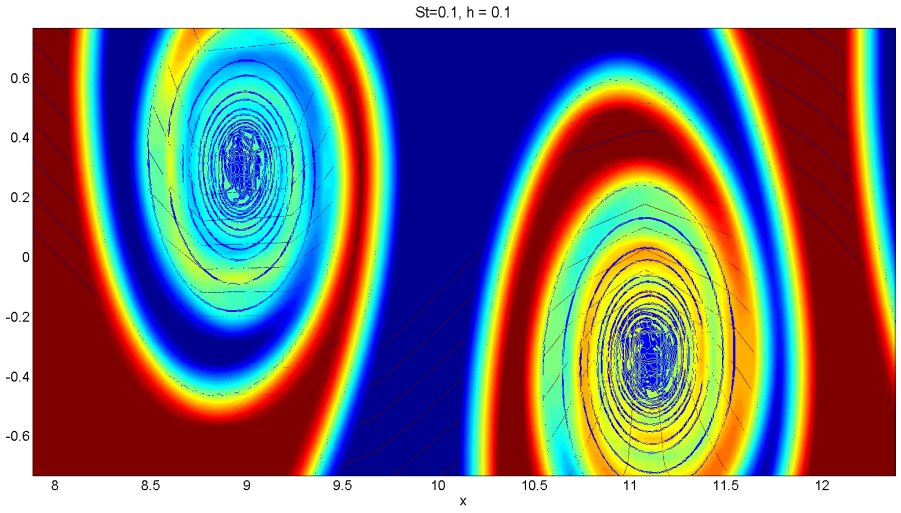
St=0.1, h = 0.1
x

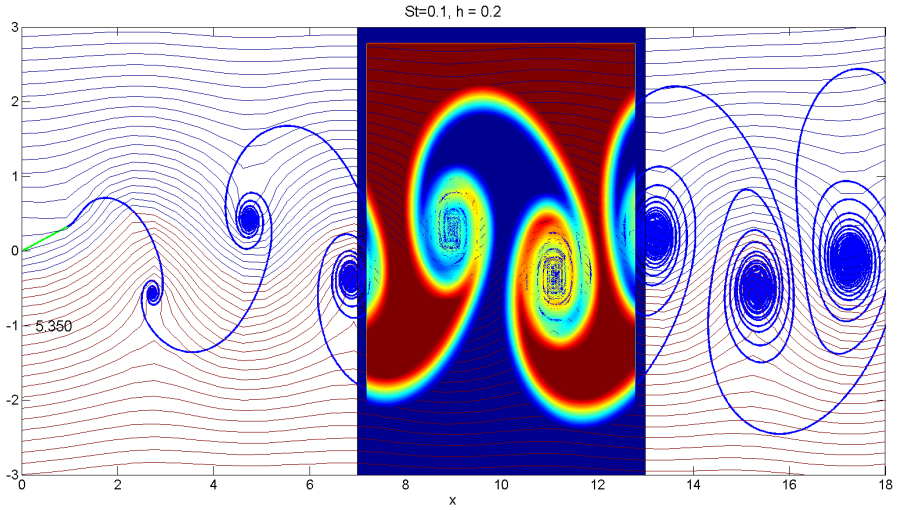
St=0.1, h = 0.2
5.350
x

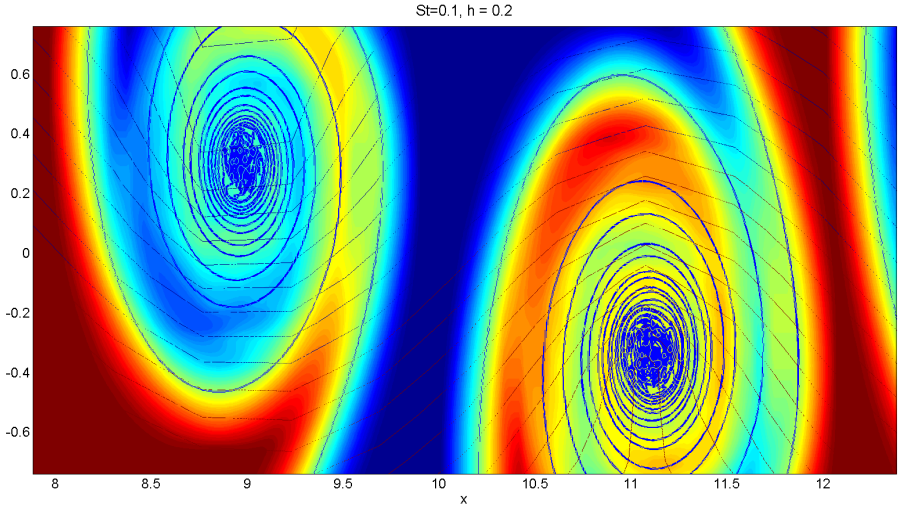
St=0.1, h = 0.2
x

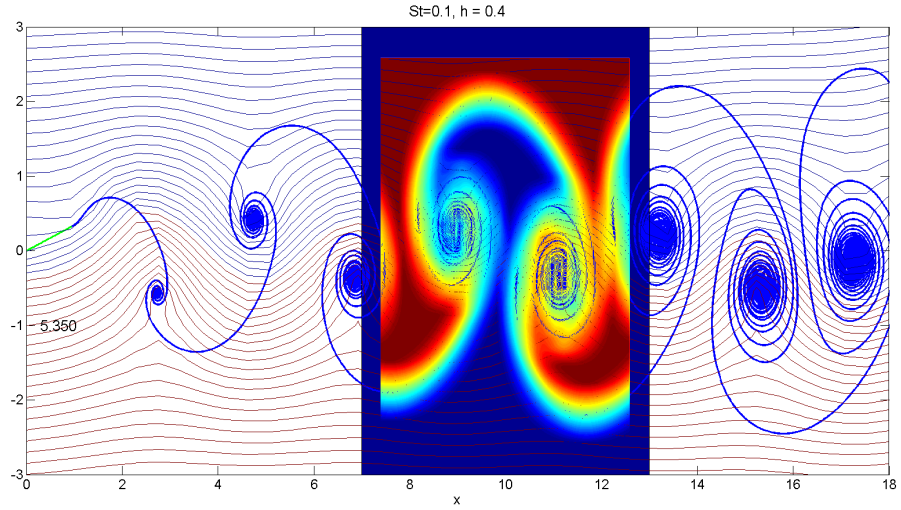
St=0.1, h = 0.4
5.350
x

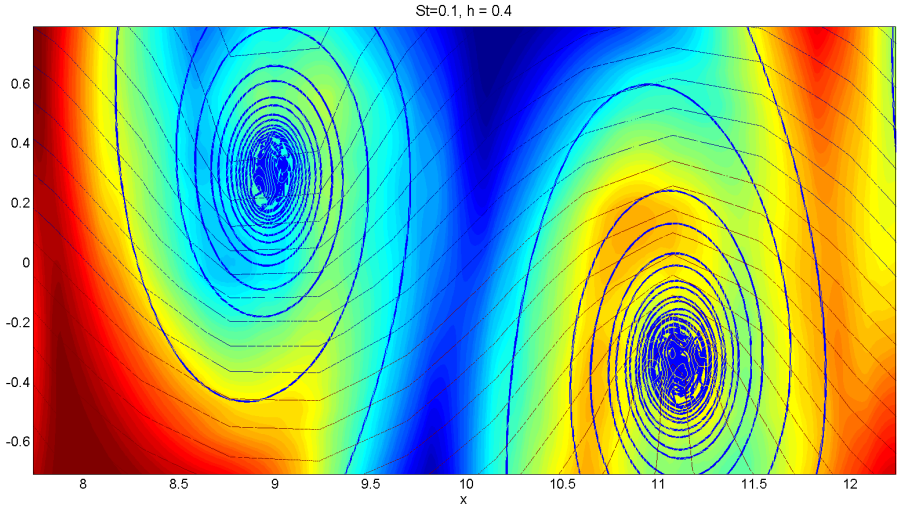
St=0.1, h = 0.4
x

Chapter 4

Particle Displacement

Having determined a measurement of mixing in our model, we then move our focus to our second goal: measuring displacement. In order to monitor and calculate the dispersion of fluid particles as they travel past the plate and become trapped within vortices, we have to add one more element to the model: a "slab" of fluid particles, placed behind the plate, which moves with the velocity of the background flow as shown in Figure 4.1. These particles will travel with the flow and, through mixing and otherwise, become displaced from their original position. We reverse the reference frame for this part of the problem, fixing the frame at infinity rather than on the plate. This analysis is also completed during post-processing, just as with the mixing results.

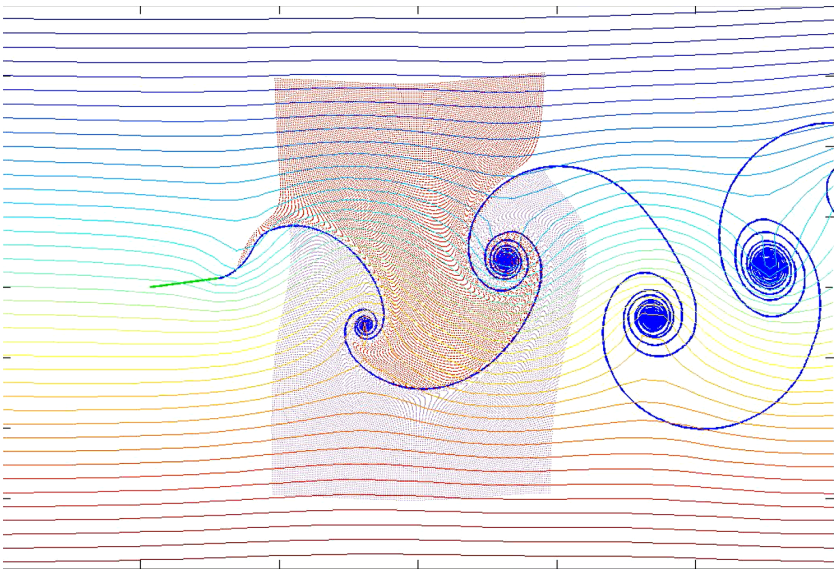

Figure 4.1: Flow with "Slab"

4.1 Our Formula

In order to measure integral displacement, we had to develop a numerical approximation. In a reference frame fixed at infinity, we replace $\mathbf{u}$ by $\mathbf{u}-\mathbf{u}_\infty$, where $\mathbf{u}_\infty$ is the constant velocity of the background flow. We denote the integral displacement as $V_d(t)$, which is dependent on time t. Our formula is:

$$\begin{aligned} V_d(t) &= \iint_R d(\mathbf{x}_0, t) d\mathbf{x}_0 \\ &\approx \sum_i \sum_j d(\mathbf{x}_{0(i,j)}, t) \Delta x \Delta y \end{aligned} \tag{4.1}$$

where $d(\mathbf{x}_0, t) = |\mathbf{x}(t; \mathbf{x}_0) - \mathbf{x}_0|$ and $\mathbf{x}(t)$ solves the differential equation

$$\begin{aligned} \frac{d\mathbf{x}}{dt} &= (\mathbf{u} - \mathbf{u}_\infty)(\mathbf{x}, t) \\ \mathbf{x}(0) &= \mathbf{x}_0 \end{aligned} \tag{4.2}$$

for every $\mathbf{x}_0$ in the "slab" of points.

4.2 The Results

We calculate V_d at every time step for seven periods to create a plot of the function in time. The result of this process can be seen in Figure 4.3, which is plotted on a log-linear scale.

We found this result surprising. The level part at the beginning details the portion of the simulation before the plate hits the slab of points. Afterwards, as we would expect, there is a sharp exponential growth in integral displacement as points become trapped in vortices and swirl away from their original positions. We hypothesized before, however, that the points would then spin back to close to their original positions and we would see a leveling off of the graph. This picture seems to mirror the shape of either a square root or logarithmic function. Both of these, though they will increase at a decreasing rate, will increase to infinity, implying that the points never reach a steady state. We know from real flows that flows absolutely must steady out - like in a pond, where ripples will eventually dissipate given enough time. We theorize that this is an issue with our model.

In addition to this function, we also decided to see where the most movement occurs. We chose to make a video of the evolution of $d(\mathbf{x}_0, t)$ at each point $\mathbf{x}_0$. As we obviously cannot include the video in this paper, refer to Figure 4.2 for three snapshots of the video at different points in time.

The blue areas refer to points that have not moved far from their original locations or, at later times, have returned to close to their original location. Yellow refers to points that have moved moderately far from their original locations, and red refers to points that have moved significantly far from

their original positions. The points in the middle of vortices have moved the furthest, whereas those which never hit the velocity and flow induced by the plate stay roughly close to their original positions. The video also shows that there seems to be a movement bias - all of the points will move together either downwards or upwards, depending on the original flapping motion of the plate. Our simulation always flaps the plate downwards first, so all of the points move downward as time progresses.

There is an alternative approach of plotting the total distance travelled, which will show different information for each particle. Some particles which have returned to close to their original positions may have actually been far away, and then come back, but travelled a large distance. Images of this phenomenon are not shown.

These snapshots help explain what we see in Figure 4.3. The points trapped in the vortices are constantly moving further and further from their original positions, and thus contribute to the continued growth of $V_d(t)$.

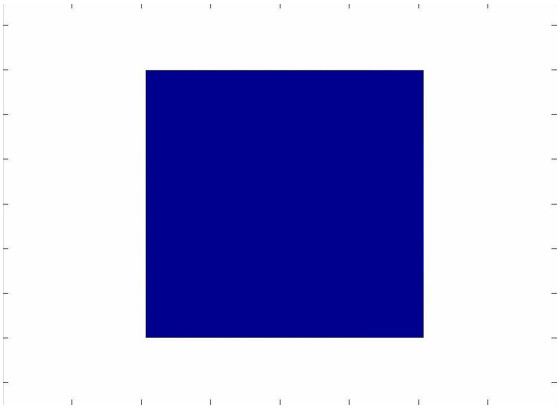

(a) At t=0

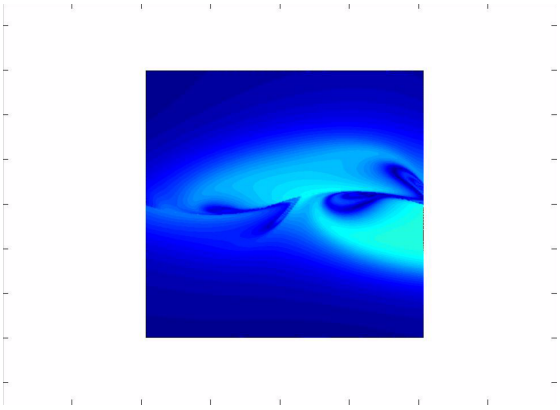

(b) After some time

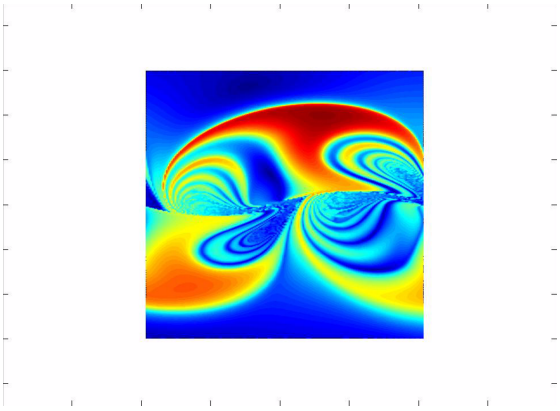

(c) At t=7

Figure 4.2: Snapshots of Evolution of Fluid Particle Displacement

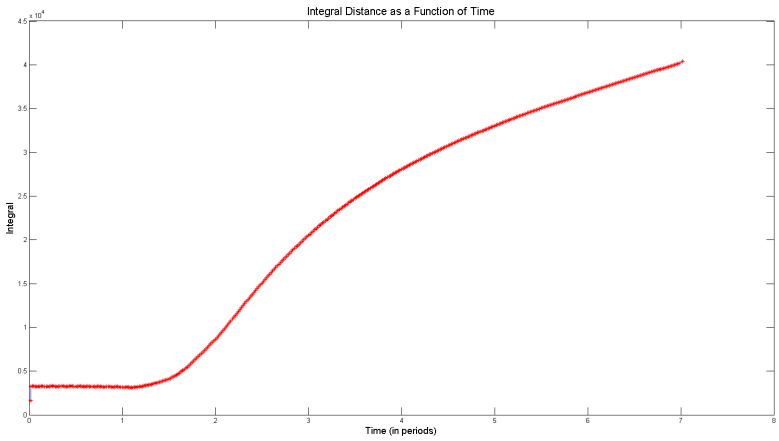

Figure 4.3: Integral Displacement as a function of time

Chapter 5

Conclusion

5.1 Summary

This paper covered the explanation and background of our problem to begin. We have a parallel background flow past an immersed plate, fixed at one end, which flaps in a prescribed motion. This model is made up of three main parts: a free vortex sheet to model the shear layer, a bound vortex sheet to model the plate, and boundary layer separation modelled by releasing a point vortex at every time step into the flow. The picture of this model is once again shown below.

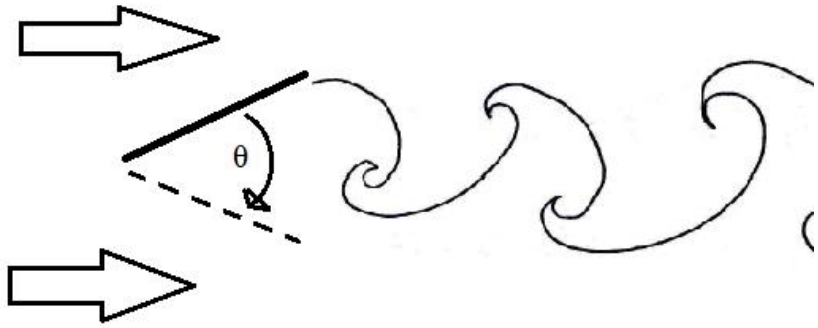

Figure 5.1: Visual of the Model

We have several findings from this work. In terms of mixing, we find exactly what we would expect - that the most mixing occurs within the vortices, where it is more intense for the larger regions of interest across the boundary of the free vortex sheet. We displayed this in several figures in Chapter 3.

Next we have more surprising results - that our simulation results in linear growth in the integral displacement function $V_d(t)$, the formula for which is given by equation (4.1). This function as plotted in Figure 4.3

appears to continue increasing, but at a seemingly decreasing rate, which may indicate that the function eventually hits a plateau. The points which show the most displacement are those in the center of the vortices, which also tend to move downwards (or upwards) depending on the movement bias of the plate. In the next section, we will talk about future work on both of these subjects and possible methods of improvement.

5.2 Future Work

To continue this work, we would ideally like to do a few things. First, our measure of mixing is rough and elementary. We would like to find a way to measure this mixing using an integral method as opposed to using proportions. As this kind of measurement has not been approached before, we feel that it is a natural step from our current work. Our current method, however, would benefit from longer runs of our simulation. Currently, we only have data up to slightly over seven periods. Due to time and computational speed and power limitations, we were unable to complete a longer run for this paper. We would like to run the simulation to at least ten periods, preferably longer, to see if we can find any other trends.

A longer run could also benefit our integral displacement analysis. At seven periods, our function $V_d(t)$ appears to continue to increase, but at a decreasing rate. This could imply either a behavior like $\sqrt{x}$ or $\log(x)$, or it could reach a plateau given enough time. If it behaves like the former, this could imply an issue with our model. We would then be inclined to research improvements to our model in which the particles would evetually reach a steady state, similar to what we see in real flows.

Bibliography

[1] A. Chorin and J. Marsden, *A Mathematical Introduction to Fluid Mechanics*, Springer-Verlag, New York, NY, third ed., 1993.

[2] K. Katija and J. Dabiri, *A viscosity-enhanced mechanism for biogenic ocean mixing*, Nature, 460 (2009), pp. 624–627.

[3] R. Krasny, *Desingularization of periodic vortex sheet roll-up*, Journal of Computational physics, 65 (1986), pp. 292–313.

[4] ——, *A study of singularity formation in a vortex sheet by the point-vortex approximation*, Journal of Fluid Mechanics, 167 (1986), pp. 65–93.

[5] J. Marsden, *Elementary Classical Analysis*, Freeman and Co., NY, 1974.

[6] M. Nitsche, *Fluids: A cool approximation of complex variables*, 2013.

[7] M. Nitsche and R. Krasny, *A numerical study of vortex ring formation at the end of a circular tube*, Journal of Fluid Mechanics, 276 (1994), pp. 139–161.

[8] J. Sheng, A. Ysasi, D. Kolomenskiy, E. Kanso, M. Nitsche, and K. Schneider, *Simulating Vortex wakes of flapping plates*, vol. 155 of The IMA Volume in Mathematics and its Applications, Springer New York, 2011.